Biochimica et Biophysica Acta 858 (1986) 243–253
Elsevier

BBA 73094

The interaction of *n*-alkanes and *n*-alcohols with lipid bilayer membranes: a ^{2}H-NMR study

J.M. Pope and D.W. Dubro

School of Physics, The University of New South Wales, P.O. Box 1, Kensington, NSW 2033 (Australia)

(Received November 20th, 1985)

Key words: Alkane-membrane interaction; Alcohol-membrane interaction; ^{2}H-NMR

The interaction of a number of *n*-alkanes and *n*-alcohols with lipid bilayers formed from dimyristoylphosphatidylcholine has been studied by ^{2}H-NMR. The ability of the *n*-alkanes to intercalate between the ordered lipid chains is strongly chain-length-dependent in both gel and liquid-crystal phases. The influence of *n*-alkane and *n*-alcohol solutes on the order of the lipid chains is also a function of solute chain-length. Short-chain *n*-alkanes are relatively insoluble in both gel and liquid-crystal phases as an ordered component.

Introduction

Lipid bilayers are a common component of biological membranes. They can be regarded as forming a matrix or substrate into which are incorporated more biochemically active constituents such as membrane-bound proteins that impart special characteristics to the bilayer and distinguish one type of membrane from another [1]. The state of the lipid bilayer regions of the membrane is determined by the composition of the constituent lipids and may be affected by the presence of lipid-soluble drugs and anaesthetics [2]. As well as influencing the properties of the bilayer itself (notably its thickness, permeability and fluidity), changes brought about by the incorporation of small lipid-soluble molecules may affect the activity of other membrane constituents such as the integral membrane proteins [3]. In an earlier study, ^{2}H-NMR and low-angle X-ray diffraction methods were employed in a study of the incorporation of several *n*-alkanes (*n*-hexane, *n*-octane, *n*-dodecane) and one *n*-alcohol (*n*-octanol) in lipid bilayer membranes formed from dimyristoylphosphatidylcholine (DMPC) at low hydration [4]. These model solutes were selected as providing the opportunity to (i) observe effects of varying solute chain-length and (ii) contrast the behaviour of purely hydrophobic *n*-alkane solutes with that of an alcohol, which contains the hydrophilic hydroxyl moiety. In addition, both classes of solute are found to exhibit anaesthetic properties, while the *n*-alkanes are commonly employed as solvents for the lipid in the formation of black lipid membranes. The latter, which are extensively used in studies of the transport properties of lipid bilayers, can be expected to contain some *n*-alkane if formed in this way.

In the present paper, we extend the work on *n*-alkane and *n*-alcohol solutes to include a range of lipid hydrations. ^{2}H-NMR methods were used to study both the ordering of the solute molecules in the bilayer and the effect of their incorporation on the order of the lipid alkyl chains, the latter by employing DMPC with perdeuterated chains. Results for *n*-butanol and *n*-hexadecane are dis-

Abbreviations: DMPC, dimyristoylphosphatidylcholine; DPPC, dipalmitoylphosphatidylcholine.

cussed as well as those solutes studied previously. In order to facilitate comparison of the data for different solutes and lipids, differential scanning calorimetry (DSC) measurements of the main gel to liquid-crystal transition have also been made. Some preliminary observations on the ordering of *n*-alkanes and *n*-alcohols in the gel phase are included.

Theory

The theory of ^{2}H-NMR as applied to labelled sites in bilayer membranes is well-established and a full discussion can be found elsewhere [5,6]. For an unoriented (powder) sample, the separation of the principal peaks in the spectrum from a given labelled site is given by:

$$\Delta\nu_Q^P = \frac{3}{4}\frac{e^2qQ}{4h}S_{C^2H}$$

where for C^2H_2 and C^2H_3 groups, the quadrupole coupling constant $(e^2qQ/h) = 170$ kHz [7]. In lipid bilayers, the order parameter S_{C^2H} for the appropriate carbon-deuterium bond at the labelled site represents an average over all the different conformations and environments which are accessed by the molecule (whether lipid or solute) on the NMR timescale [4]:

$$S_{C^2H} = \sum_\alpha P_\alpha S^\alpha_{C^2H}$$

where P_α is the probability of conformation α. Moreover, when, as in this study, perdeuterated molecules are employed, the overall spectrum represents a superposition of powder spectra for each of the (inequivalent) ^{2}H-labelled sites. In such circumstances, computer simulation of the resulting spectra can greatly assist in their interpretation and peak assignments [4]. No attempt was made to relate the measured order parameters for the C-^{2}H bonds to a molecular or segmental order parameters, S_{mol} [5], since this pre-supposes a predominant conformation for the molecule. Such an assumption is unlikely to be valid at least for the case of solutes in lipid bilayers which diffuse rapidly between different bilayer locations.

Materials and Methods

Synthetic lipid (DMPC) was obtained from Sigma or Calbiochem. Deuterated solutes were purchased from MSD Isotopes (Canada), while the lipid with perdeuterated chains DMPC-d_{54} was obtained from Serdary Research Laboratories. The purity of the lipids was checked by TLC prior to sample preparation. Details of the latter have been given in a previous publication [4].

^{2}H-NMR spectra were recorded on a Bruker CXP-300 NMR spectrometer operating at 46.063 MHz using the $90°-\tau-90°_{90}$ quadrupolar echo technique [6]. For the liquid-crystal (L_α) phase spectra, a pulse spacing $\tau \approx 50-100$ μs was employed, but for the gel phase it was found necessary to reduce this value to approx. 30 μs. DSC measurements were made on a Perkin-Elmer differential scanning calorimeter, normally at a heating rate of 5 Cdeg/min. While this produced significant broadening of the transitions for pure lipid samples, it was found to be adequate for observing the broader transitions of the ternary systems under study here.

Results

Fig. 1 shows sets of typical ^{2}H-NMR spectra for perdeuterated solutes (*n*-hexane, *n*-dodecane and *n*-octanol), in DMPC bilayers at temperatures spanning the gel to liquid-crystal transition region. Spectral simulations are included for the highest temperature spectra, corresponding to samples which are wholly in the L_α phase. In the case of *n*-octanol, a simulation of a spectrum obtained just below the main thermal transition has also been included. Spectra from *n*-octane, *n*-hexadecane and *n*-butanol for both gel and liquid-crystal phases are shown in Fig. 2. At temperatures above the chain-melting transition, all the solutes exhibit well-resolved ^{2}H-NMR powder spectra, particularly at low lipid hydrations, indicating that while the solutes are ordered by incorporation in the lipid bilayer, their conformational motions are rapid on the ^{2}H-NMR timescale (approx. 10^{-5} s). Plots of the temperature dependence of the resolved ^{2}H-NMR splittings through the transition region for several of the samples are shown in Fig. 3.

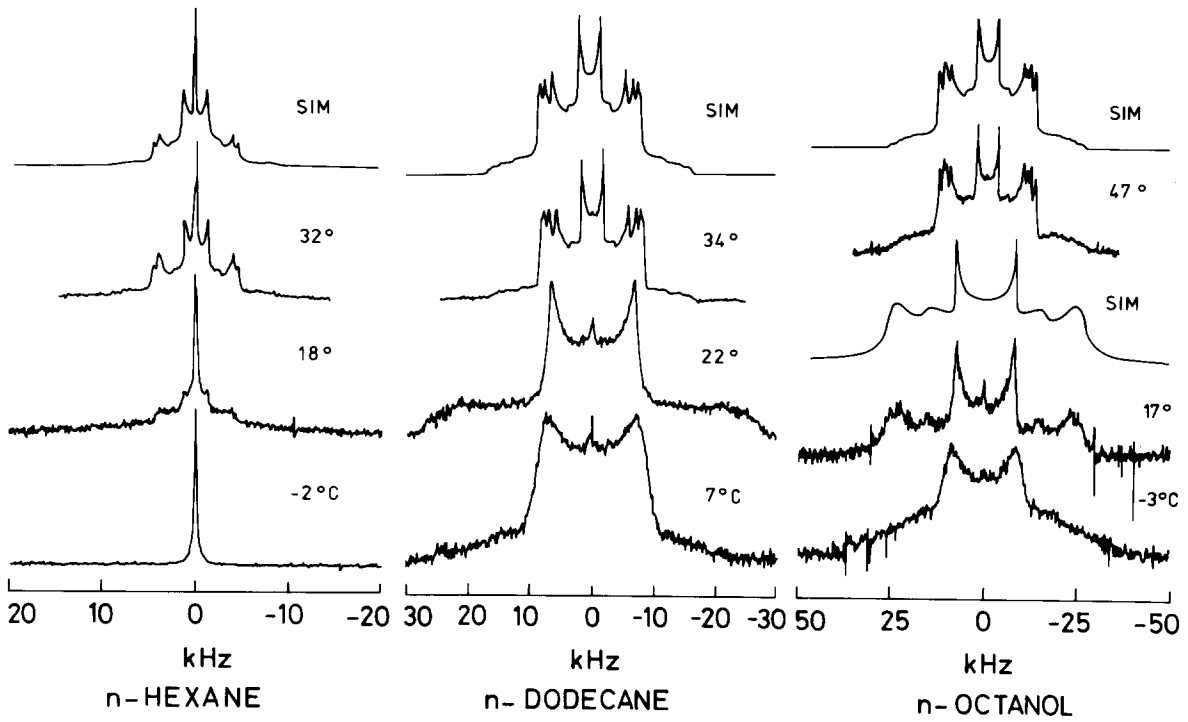

Fig. 1. ^{2}H-NMR spectra from perdeuterated solutes in DMPC bilayers. Three spectra are shown for each solute, one above and two below the gel to liquid-crystal phase transition. Samples shown are DMPC/25 H_2O/0.1 *n*-hexane-d_{14}, DMPC/9 H_2O/0.2 *n*-dodecane-d_{26} and DMPC/9 H_2O/0.4 *n*-octanol-d_{17}. Computer-simulated (SIM) spectra are also shown in selected cases.

All the solutes studied broaden the main gel to liquid-crystal thermal transition, T_m, as well as shifting its temperature in general. In the presence of excess water, short-chain *n*-alkanes and *n*-alcohols reduce T_m, while the longer-chain solutes give rise to an increase in T_m [8–10,25]. Our results show that similar changes occur at the reduced hydrations employed here. In comparing

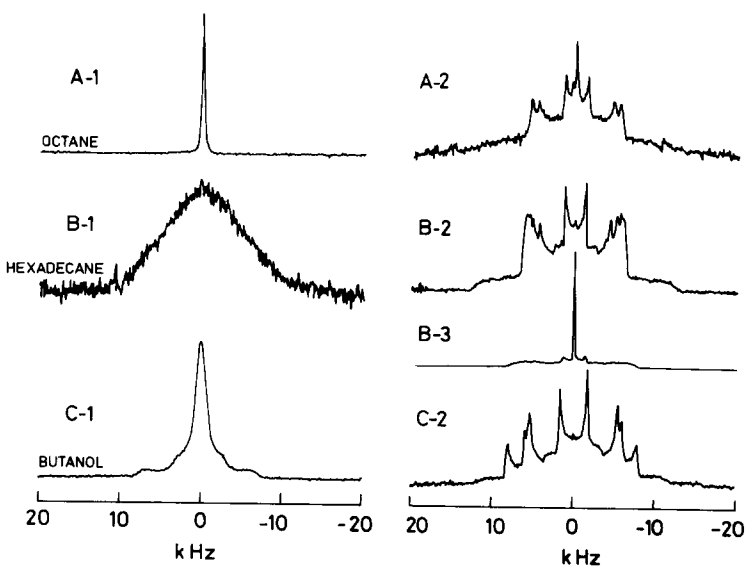

Fig. 2. ^{2}H-NMR spectra for perdeuterated solutes in DMPC bilayers in the gel and liquid crystal phases. (A) DMPC/9 H_2O/0.2 *n*-octane-d_{18} at 7 and 37°C, respectively; (B-1) and (B-3) DMPC/9 H_2O/0.2 *n*-hexadecane-d_{34} at 7 and 35°C, (B-2) 0.1 *n*-hexadecane-d_{34} at 40°C; (C) DMPC/9 H_2O/0.4 *n*-butanol-d_9 at 2 and 37°C.

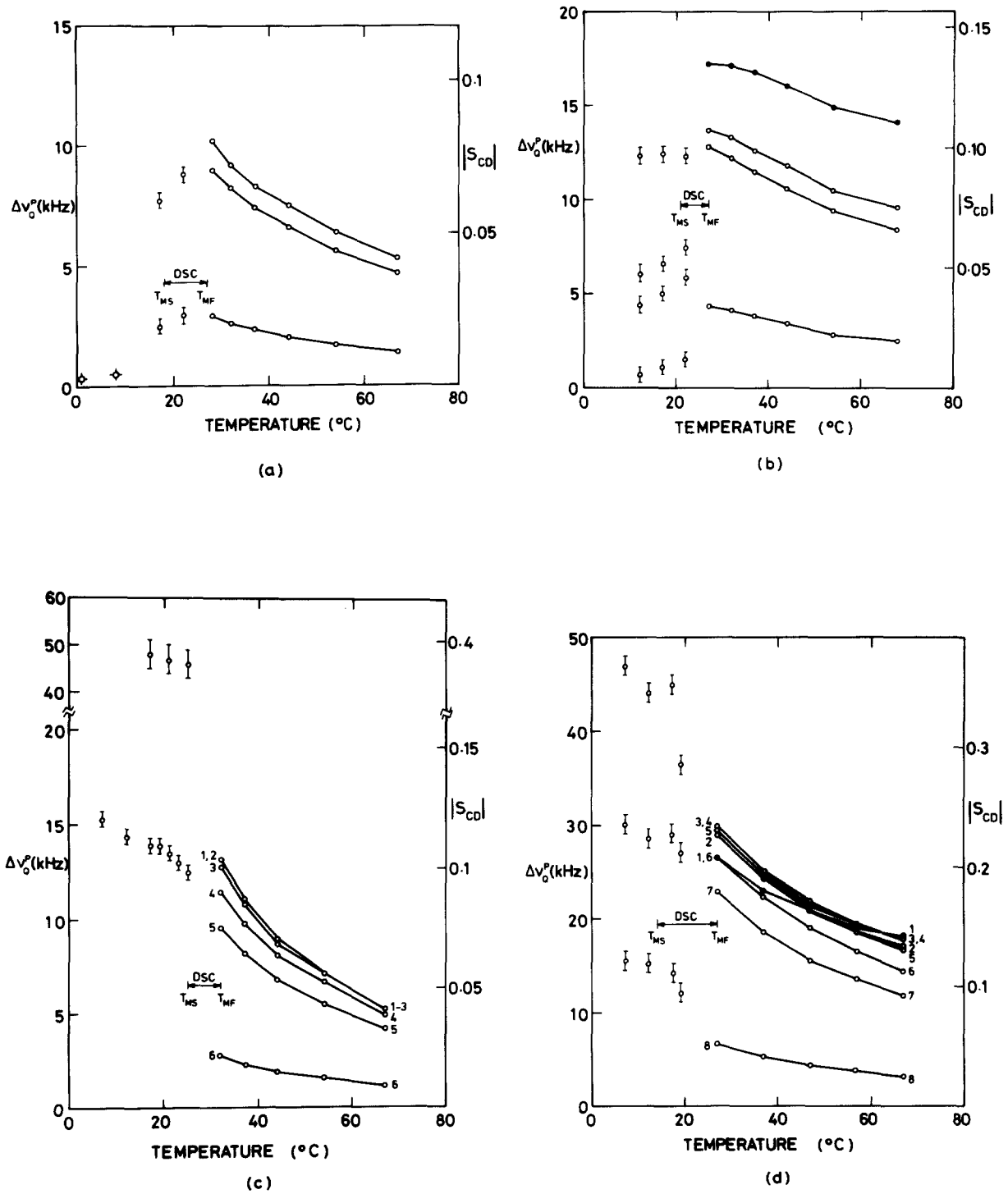

Fig. 3. Temperature dependence of ^{2}H-NMR splittings for perdeuterated solutes in DMPC bilayers. Splittings corresponding to the L_α phase are derived from spectral simulations. Chemically shifted splittings are denoted by ●, while ○ denotes FWHM for the isotropic peak derived from *n*-hexane in the low-temperature gel phase. Limits of the thermal transition measured by DSC are also indicated. (a) DMPC/25 H_2O/0.1 *n*-hexane-d_{14}; (b) DMPC/9 H_2O/0.4 *n*-butanol-d_9; (c) DMPC/16 H_2O/0.2 *n*-dodecane-d_{26}; (d) DMPC/16 H_2O/0.4 *n*-octanol-d_{17}.

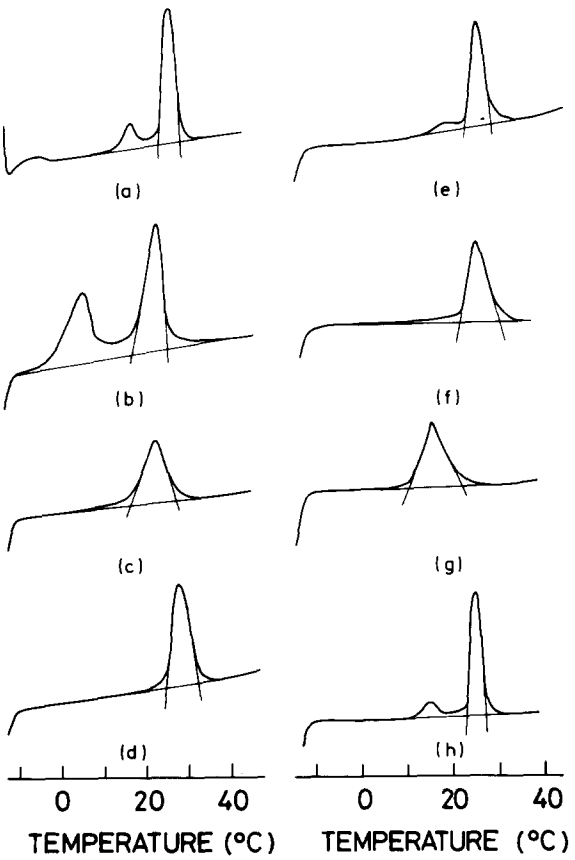

Fig. 4. DSC thermograms of the gel to liquid-crystal transition in DMPC bilayers containing various solutes. (a) DMPC/16 H_2O; (b) DMPC/16 H_2O/0.1 *n*-hexane; (c) DMPC/16 H_2O/0.2 *n*-octane; (d) DMPC/16 H_2O/0.2 *n*-dodecane; (e) DMPC/16 H_2O/0.1 *n*-hexadecane; (f) DMPC/9 H_2O/0.4 *n*-butanol; (g) DMPC/25 H_2O/0.4 *n*-octanol; (h) DMPC/25 H_2O. Starting and finishing temperatures (T_{ms} and T_{mf}) of the main thermal transition were determined as indicated on the thermograms.

TABLE I

EFFECT OF SOLUTES ON THE MAIN THERMAL TRANSITION IN DMPC BILAYERS

Starting and finishing temperatures (T_{ms} and T_{mf}) are given in each case in °C. (See text for details.)

Bilayer composition	Lipid hydration		
	$n = 9$	$n = 16$	$n = 25$
Pure DMPC	28 –34	24.2–29.5	23.2–27.8
DMPC/0.1 *n*-hexane	21 –28.5	18 –26.5	18 –27
DMPC/0.2 *n*-octane	21.5–29.2	17.8–28	17.2–25
DMPC/0.2 *n*-dodecane	25.3–32.8	25 –32.2	24.3–31.5
DMPC/0.1 *n*-hexadecane	26.3–34	25.3–30.3	25 –29.5
DMPC/0.4 *n*-butanol	23.3–32.7		
DMPC/0.4 *n*-octanol	23 –32.1	14 –27	11 –24

the effects of solute concentration or lipid hydration on the order and mobility of both the solute molecules themselves and the bilayer in which they are dissolved, it is important to determine the magnitude of such changes in chain-melting temperature. This information is also necessary in making comparisons of different solutes or assessing the influence of changes in lipid chain-length. Further, it can provide valuable additional insights into the solubility, location and behaviour of different solutes in the bilayer. While changes in T_m are apparent from the ^{2}H-NMR results themselves, such data can be obtained more efficiently from differential scanning calorimetry. Typical DSC thermograms are shown in Fig. 4, which also demonstrate our criterion for determining the width of the main transition region [8], as defined by the starting and finishing temperatures, T_{ms} and T_{mf}. This range is also indicated on the plots of Fig. 3 and values are given in Table I.

For each of the solutes studied, measurements were made at lipid (DMPC)/water molar ratios of 1 : 9, 1 : 16 and 1 : 25, the latter corresponding to excess water [11,12]. In all cases, the quadrupole splittings decrease monotonically with increasing temperature in the L_α phase (Fig. 3), reflecting increased molecular mobility and reduced order. For the *n*-alkane solutes, the maximum number of resolved splittings was half the number of segments in the alkyl chain, confirming that these molecules retain the equivalence of segments equidistant from the molecular centre when ordered in the bilayer environment. This can be explained if the molecules shuffle rapidly back and forth across the bilayer centre and/or experience end-for-end flips within a monolayer in the L_α phase. In contrast, for the *n*-alcohols, the maximum number of splittings required to adequately simulate the solute spectra corresponded to the chain-length, confirming that the frequency of such motions is greatly reduced by the affinity of the hydroxyl group for the aqueous interface region of the bilayer.

Assignment of the resolved slittings to molecular segments is aided by the computer simulations and has been discussed in detail previously [4]. Briefly, in the case of the *n*-alkanes, it was assumed that segmental order decreases monotonically away from the molecular centre, while for

the *n*-alcohols the assignments are facilitated by an observable chemical shift for the deuterons nearest the hydroxyl terminal, and in the case of *n*-octanol an anomalous temperature dependence of the ^2H splittings for the first few segments down the chain (Fig. 3d). On the basis of these assignments, order parameter profiles can be calculated for each of the solutes studied. In comparing such profiles, it is of interest to attempt to separate effects resulting from changes in conformational motion of the solutes from those resulting from an overall change in molecular order. The former imply a qualitative change in the motion of the solute while the latter can be expected largely to reflect changes in the average order of the surrounding lipid bilayer matrix. Since it is these changes which also give rise to the observed shifts in chain-melting temperature, T_m, we have compared order parameters for different samples on the basis of a reduced temperature ($T - T_{mf}$), where T_{mf} is the temperature above which the sample is wholly in the L_α phase. Profiles for several of the solutes investigated are compared in this way in Fig. 5, where the effects of lipid hydration and solute concentration on solute order are also shown.

Representative spectra from bilayers formed from chain perdeuterated DMPC, both in the presence and absence of solutes are shown in Fig. 6. Spectral simulations for pure DMPC-d_{54}/9 H_2O bilayers are based on peak assignments for dipalmitoylphosphatidylcholine (DPPC) bilayers [13] which were in turn derived from data for selectively deuterated lipids. Modification of the assignments for the difference in chain-length between DPPC and DMPC appears straightforward.

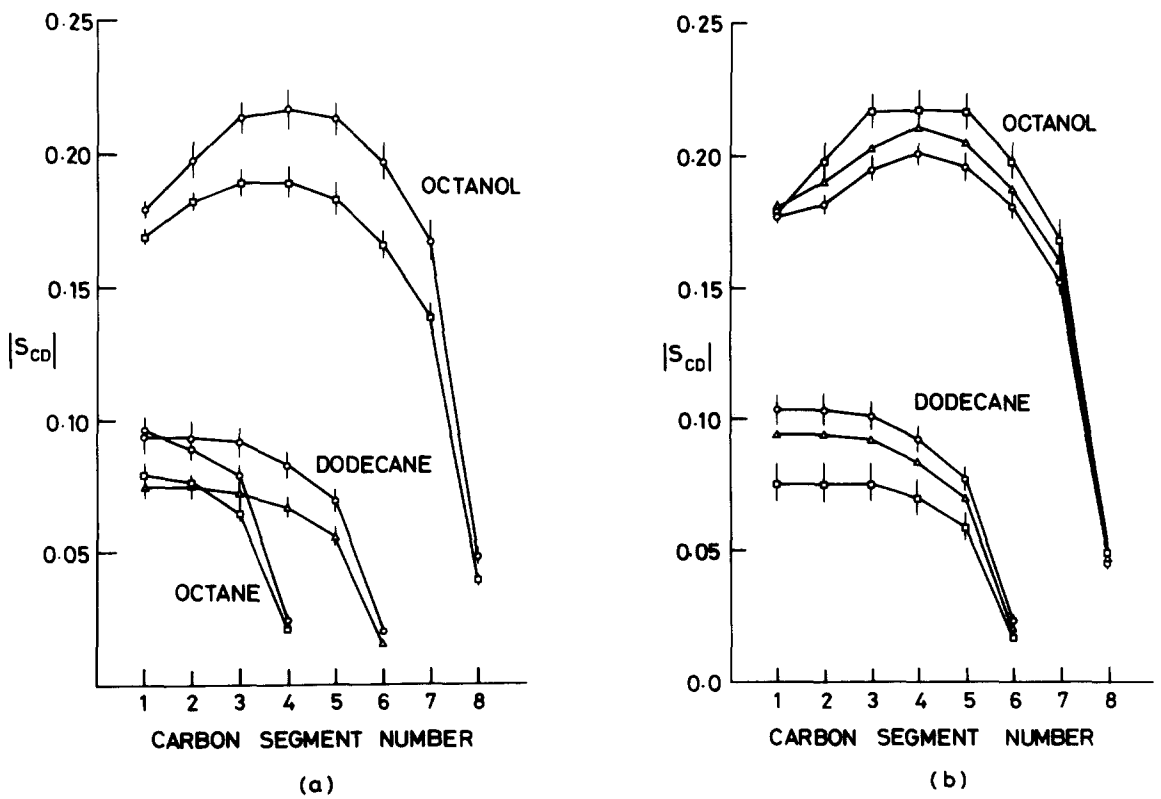

Fig. 5. Order parameter profiles for different solutes showing the influence of hydration and solute concentration. All profiles are at 10 Cdeg above T_{mf}. Error bars (on extremum curves) indicate deviations of ±2 Cdeg in the determination of T_{mf}. (a) Influence of hydration on order parameter profiles for bilayers of composition DMPC/*n* H_2O/0.2 octane-d_{18}, DMPC/*n* H_2O/0.2 dodecane-d_{26} and DMPC/*n* H_2O/0.4 octanol-d_{17} with $n = 9$ (○), $n = 16$ (△) and $n = 25$ (□); (b) Influence of solute concentration for bilayers of composition DMPC/9 H_2O/*X* *n*-dodecane-d_{26} and DMPC/9 H_2O/*X* *n*-octanol-d_{17} with $X = 0.1$ (○); $X = 0.2$ (△) and $X = 0.4$ (□).

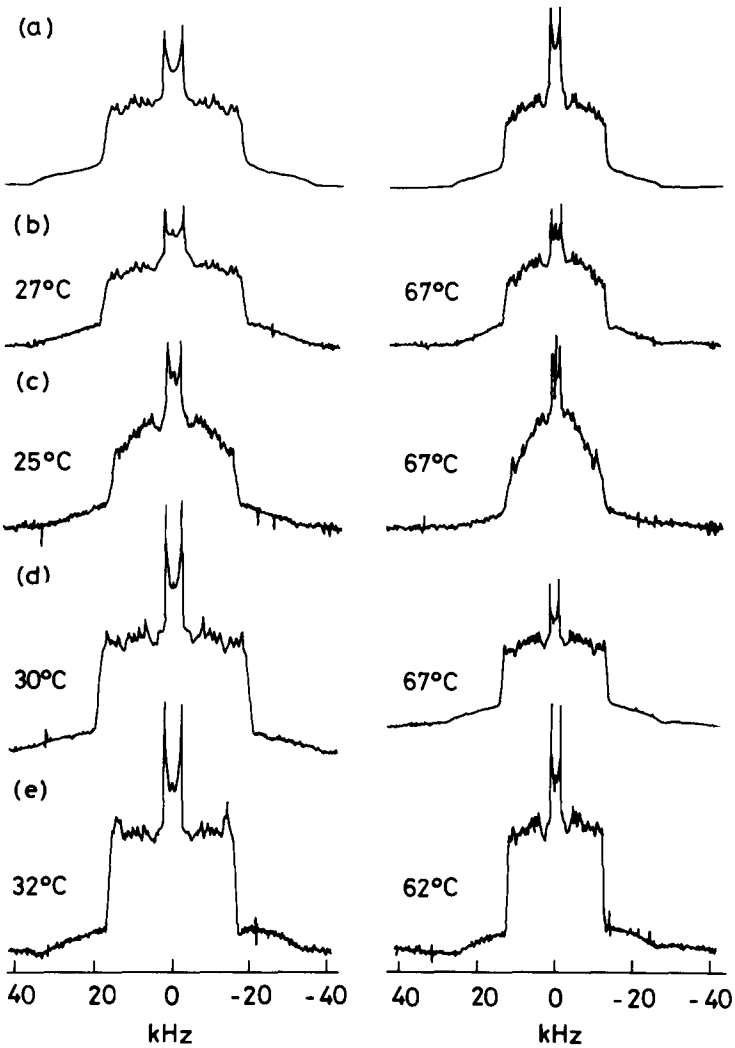

Fig. 6. ^{2}H-NMR spectra for perdeuterated lipids in different lipid-solute systems at the temperatures indicated. (a) Simulations of DMPC-d_{54}/9 H_2O; (b) DMPC-d_{54}/9 H_2O; (c) DMPC-d_{54}/9 H_2O/0.6 *n*-butanol; (d) DMPC-d_{54}/9 H_2O/0.4 *n*-octanol; (e) DMPC-d_{54}/9 H_2O/0.2 *n*-dodecane.

Changes in the spectra on addition of the solutes can be substantial and in general prevent a complete assignment of the splittings in these cases. This would require spectra from samples containing selectively deuterated lipids in the presence of the solutes. However, it is clear that the central resolved splitting reflects the order of the terminal C^2H_3 groups of the lipid chains, while the outer edges of the main part of the spectrum yield the order parameter for the most ordered segments of the acyl chains. In addition, experience with simulation of the spectra from solute-free bilayers shows that the shape of the overall spectrum is sensitive to the number of chain segments contributing to the order parameter plateau [5,6]. The latter arises from segments near the glycerol back-

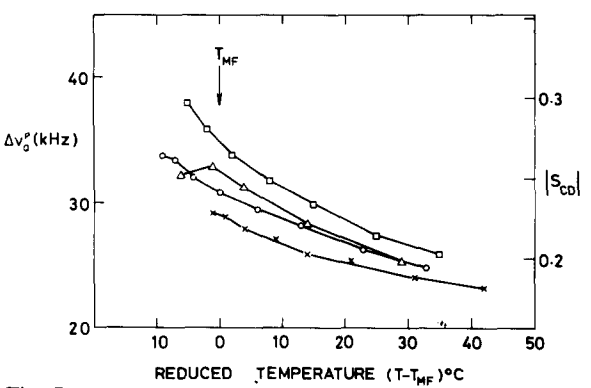

Fig. 7. Temperature dependence of the width of ^{2}H-NMR spectra (FWHM) for perdeuterated lipids with different solutes plotted against reduced temperature ($T - T_{mf}$). ○, DMPC-d_{54}/9 H_2O; (□) DMPC-d_{54}/9 H_2O/0.4 *n*-octanol; △, DMPC-d_{54}/9 H_2O/0.2 *n*-dodecane; ×, DMPC-d_{54}/9 H_2O/0.6 *n*-butanol.

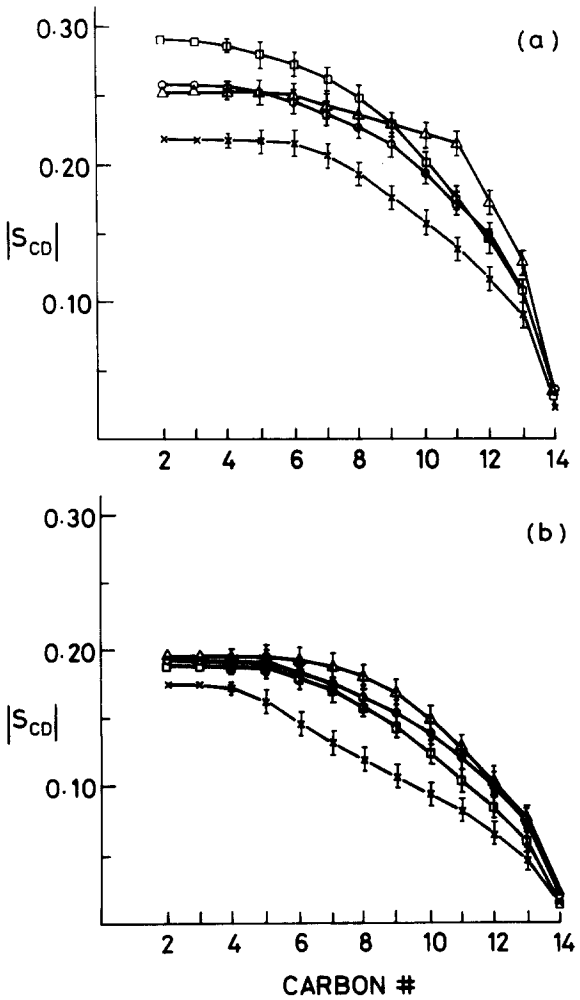

Fig. 8. Order parameter profiles for DMPC/9 H_2O bilayers with perdeuterated lipid chains in the presence of solutes. Order parameters were obtained by simulation of the spectra of Fig. 6, and the method of assignment is outlined in the text. Temperatures were (a) just above the main chain-melting transition and (b) approx. 30 Cdeg above T_m; ○, solute free; □, 0.4 *n*-octanol; △, 0.2 *n*-dodecane; ×, 0.6 *n*-butanol.

bone region of the bilayer (although the 2-positions exhibit anomalous behaviour) and is most marked just above the gel to liquid-crystal transition [14]. The temperature dependence of splittings corresponding to this plateau is shown for several samples with and without solutes in Fig. 7. By comparison, the solutes had little effect on the splittings for the terminal methyl-end of the chains, when corrected for changes in T_{mf}. Finally, order parameter profiles obtained from simulations of the spectra of Fig. 6 are compared in Fig. 8, where the error bars reflect the degree of uncertainty in assignment of the individual peaks mentioned above. Points corresponding to those 2-positions which yield anomalous splittings have also been omitted from Fig. 8.

Discussion

L_α phase

Previous studies [8–10,15–20,25] have shown that *n*-alkanes C_6–C_{16} and *n*-alcohols C_3–C_{18} dissolve in lipid bilayers to varying degrees, without producing gross changes in bilayer structure. Data on the location of the solutes within the bilayer and the extent to which they intercalate between the lipid chains is however much more limited [4,10,19,20]. Results on black lipid membranes [15–17] indicate that the solubility of *n*-alkanes in the L_α phase decreases with increasing chain-length, with a sharp cut-off in solubility around C_{14} for bilayers in the absence of cholesterol. The present data confirm that hexadecane is relatively insoluble in DMPC bilayers above the phase transition, as evidenced by the emergence of an isotropic peak in spectra from the deuterated solute at molar ratios n' (solute/DMPC) above 0.1 (Fig. 2). A central peak in these spectra reflects the presence of a separate component reorienting isotropically and in slow exchange with the ordered component. This is in contrast to *n*-dodecane, for which no significant isotropic component is evidenced at concentrations up to $n' = 0.4$, at least at low hydrations. (A small central peak in all the spectra, especially at higher hydrations, reflects the presence of natural abundance ^{2}HHO in the water). More surprising is the presence of an isotropic peak in the spectra from *n*-hexane at concentrations as low as $n' = 0.1$, indicating that there is an optimum chain-length for *n*-alkanes to intercalate between the lipid chains of about C_{12} in DMPC. Both shorter- and longer-chain *n*-alkanes appear less able to mix with the lipid chains of the bilayer. No such isotropic components were observed in the ^{2}H-NMR spectra of *n*-butanol ($n' = 0.6$) and *n*-octanol ($n' = 0.4$).

That the powder ^{2}H spectra result from solute molecules intercalated between the alkyl chains of the lipid molecules (rather than forming an ordered sandwich between monolayers at the bilayer

centre) is evidenced by the order parameter profiles of Fig. 5. In the case of *n*-octanol, the magnitudes of the ^2H splittings from the most ordered segments (Fig. 1) are comparable to those of the lipid chain (Fig. 6), while the presence of a significant order parameter plateau, especially at temperatures well above the phase transition, reflects that exhibited by the lipid chains (Refs. 5, 6, 14, and Fig. 8). This confirms that, as expected, the terminal hydroxyl group is anchored near the aqueous interface. At temperatures just above T_m, the polar hydroxyl group may project significantly into the aqueous phase, beyond the most ordered 'glycerol backbone' region of the bilayer, giving rise to a reduced order parameter for this segment (Fig. 5). Similar effects have been observed for *n*-decanol in soap bilayers [21,22]. Anchoring of the hydroxyl group at the aqueous interface of the bilayer is also reflected in a approx. 25% increase in order parameter for the terminal methyl group with respect to that for the acyl chain methyls of the lipid molecules. This results from the shorter length of the *n*-octanol chain so that the alcohol methyl groups are pulled into more ordered regions of the lipid bilayer [14].

Order parameters for the *n*-alkanes are much lower than those for the *n*-alcohols (Fig. 5), since these non-polar molecules prefer the more disordered hydrophobic interior of the bilayer. We believe, however, that here too the ordered component arises from molecules oriented between the lipid chains, since for the long-chain *n*-alkanes, segments near the molecular centre exhibit similar order parameters. Very different order profiles are expected and indeed observed for long-chain alkanes solubilized in a lamellar phase between the monolayer, where there is little mixing of alkane and lipid chains [23]. Further, in the case of *n*-hexane in DMPC bilayers, Jacobs and White [20] have recently shown from the orientation dependence of the solute ^2H splittings in macroscopically oriented bilayers, that the symmetry axis for motional averaging of both alkane and lipid chains is the bilayer normal. Additional evidence for this model of alkane ordering in lipid bilayers comes from X-ray data [4,18] which shows that the *n*-alkanes increase bilayer area as well as thickness (although their effect on area is less than that of the *n*-alcohols). Such results indicate that the cut-off in solubility at long chain-length exhibited by both *n*-alkanes and *n*-alcohols does not, as suggested by Janoff and Miller [2], occur at the chain-length where the solutes begin to align with the lipid chains.

The precise nature of the isotropic components in the spectra of both short- and long-chain *n*-alkanes remains unclear. While it almost certainly arises from solute molecules forming an isotropic phase in the bilayer centre, this is unlikely to take the form of a uniform layer between the monolayers, since the molecules forming such a layer would be expected to exchange rapidly with the ordered component [4]. A more plausible explanation is that the excess *n*-alkane forms 'lenses' or vesicles containing bulk *n*-alkane enclosed by a lipid monolayer. It is worth noting at this point that the solubility of *n*-hexane as an ordered component ($n' < 0.1$) appear lower in our unoriented samples than that observed by Jacobs and White ($n' \approx 0.24$) for planar oriented samples [20]. This lends some support to the suggestion of Gruen and Haydon [24] that the solubility of the *n*-alkanes in lipid bilayers may be curvature-dependent. It is known to be high for short-chain *n*-alkanes in planar black lipid membranes [15–17], although in this case the state of order of the *n*-alkane retained in the bilayer is unknown.

In all cases studied here, increasing lipid hydration results in a reduction in solute order (Fig. 5a), reflecting the reduction in average order of the lipid chains in the bilayer associated with an increased area per lipid molecule. Increasing solute concentration at fixed lipid hydration also results in a reduction in average solute order for the *n*-alkanes and *n*-butanol, but in the case of *n*-octanol the reverse is true, the average order of the solute molecules increasing as the solute concentration is increased (Fig. 5b). These results can be interpreted in terms of a model in which the *n*-alkanes initially occupy most favourable 'sites' in the bilayer with minimum disruption of bilayer order, but as the solute concentration is increased, less favourable sites become occupied with greater disruption in packing of the lipid chains. In contrast, the hydroxyl terminals of the *n*-octanol molecules are anchored at the aqueous interface region and the alkyl chains extend into the bilayer between the lipid chains, restricting the range of

conformations accessible to them and increasing the average bilayer order. Such effects are not observed for *n*-butanol because of the shortness of the alkyl chain in this case and the fact that this water-soluble molecule partitions between the bilayer and the aqueous phase. For the same reasons, order parameter profiles calculated from the data of Fig. 3b do not show an order parameter plateau for *n*-butanol.

Further evidence for this picture of molecular packing of the solute molecules in the L_α phase is obtained from the data of Figs. 7 and 8 for the effect of the solutes studied on lipid chain order. From Fig. 7 it is clear that *n*-octanol increases the splittings of the outermost peaks of the powder spectra from bilayers comprising perdeuterated DMPC, corresponding to increased order in the 'plateau' arising from chain segments near the glycerol backbone region of the bilayer. In contrast, *n*-butanol gives rise to a reduction in order in this region. A more detailed picture is seen in Fig. 8, where the lipid order parameter profiles in the presence of solutes are compared. At temperatures close to the chain-melting transition (Fig. 8a), the increase in order produced by *n*-octanol and reduction due to *n*-butanol are seen to extend along most of the length of the lipid chains, although the effect becomes negligible at the methyl terminal. In contrast, the main effect of *n*-dodecane appears to be an extension of the order parameter plateau to chain segments further from the glycerol backbone. Similar effects are observed at higher temperatures, where it is clear that the effect of *n*-butanol on the order parameter plateau is the reverse of that produced by *n*-dodecane. This short molecule anchored at the aqueous interface gives rise to an increase in bilayer area which the lipid chains accommodate by disordering below those segments directly affected by the presence of the solute.

Gel phase

At sufficiently low temperatures in the gel phase, the short-chain *n*-alkanes are virtually insoluble in the lipid bilayer, as evidenced by the absence of a broad component in the gel-phase ^{2}H-NMR spectra from samples containing *n*-hexane (Fig. 1) and *n*-octane (Fig. 2). It would appear that, as the lipid alkyl chains solidify, these alkanes, which only exhibit low solubility as an ordered component in the L_α phase, are expelled from the bilayers to form a separate phase which probably consists of almost pure bulk *n*-alkane. This view is supported by the fact that, as the temperature is increased towards the transition, the samples pass through a mixed phase region in which ^{2}H-NMR splittings from the solutes emerge and increase with increasing temperature up to the finishing temperature of the main chain-melting transition (Fig. 3a). The increase in splittings with temperature can be explained by the alkanes exchanging rapidly between bulk liquid and those neighbouring regions of lipid bilayer which melt first. As more of the lipid bilayers melt, the proportion of time that a given solute molecule spends in the bilayer as an ordered component will therefore increase, giving rise to increased average molecular order and increased splittings, as predicted by Eqns. 1 and 2. Similar results are obtained for *n*-butanol, although in this case the solute expelled from the bilayers presumably enters the aqueous channel, where it retains some order.

In contrast, the long-chain alkanes and *n*-octanol appear to remain between the lipid chains in the gel phase. At temperatures just below the main transition, splittings from the methyl terminal and methylene segments can be resolved, consistent with a model in which the solute chains are stiff so that all the methylene segments are approximately equivalent (Fig. 1). The ratio of these splittings is approx. 1 : 3, consistent with rapid rotation of the methyl rotors about their 3-fold axis at these temperatures. At lower temperatures, the spectra broaden and the splittings from the methylene groups become unresolved, probably due to the onset of chain tilt with respect to the bilayer normal in the gel phase. The broad, unresolved spectrum obtained for *n*-hexadecane in the gel phase contrasts with that for *n*-dodecane and results from solidification of bulk *n*-hexadecane (m.p. 18°C) excluded from the bilayers.

Conclusions

Our results provide detailed support for a picture of the incorporation of *n*-alkanes and *n*-alcohols in lipid bilayers at the molecular level. At

low concentrations, both *n*-alkanes and *n*-alcohols dissolve in the L_α phase as an ordered component between the lipid chains, without inducing gross changes in bilayer structure. The ability of the *n*-alkanes to mix with the lipid chains is however strongly chain-length-dependant and in the case of the short-chain *n*-alkanes, at least, may be a function of bilayer curvature. Below the main chain-melting temperature, the short-chain *n*-alkanes are excluded from the bilayers, forming a separate alkane-rich isotropic phase.

Acknowledgement

The authors wish to acknowledge support for this work from the Australian Research Grants Scheme.

References

1 Singer, S.J. and Nicolson, G.L. (1972) Science 175, 720–731
2 Janoff, A.S. and Miller, K.W. in (1982) Biological Membranes (Chapman, D., ed.), Vol. 4, pp. 417–476, Academic Press, London
3 Israelachvili, J.N., Marcelja, S. and Horn, R.G. (1980) Q. Rev. Biophys. 13, 121–200
4 Pope, J.M., Walker, L.W. and Dubro, D. (1984) Chem. Phys. Lipids 35, 259–277
5 Seelig, J. (1977) Q. Rev. Biophys. 10, 353–418
6 Davis, J.H. (1983) Biochim. Biophys. Acta 737, 117–171
7 Burnett, L.J. and Muller, B.H. (1971) J. Chem. Phys. 55, 5829–5831
8 Eliasz, A.W., Chapman, D. and Ewing, D.F. (1976) Biochim. Biophys. Acta 448, 220–233
9 MacDonald, A.G. (1978) Biochim. Biophys. Acta 507, 26–37
10 McIntosh, T.J., Simon, S.A. and MacDonald, R.C. (1980) Biochim. Biophys. Acta 597, 445–463
11 Finer, E.G. and Darke, A. (1974) Chem. Phys. Lipids 12, 1–16
12 Pope, J.M. and Cornell, B.A. (1979) Chem. Phys. Lipids 24, 27–43
13 Davis, J.H. (1979) Biophys. J. 27, 339–358
14 Gruen, D.W.R. (1982) Chem. Phys. Lipids 30, 105–120
15 White, S.H. (1977) Ann. N.Y. Acad. Sci. 303, 243–265
16 Haydon, D.A., Hendry, B.M., Levinson, S.R. and Requena, J. (1977) Biochim. Biophys. Acta 470, 17–34
17 Haydon, D.A., Hendry, B.M. and Levinson, S.R. (1977) Nature 268, 356–358
18 Lea, E.J.A. (1979) Int. J. Biol. Macromol. 1, 185–187
19 White, S.H., King, G.I. and Cain, J.E. (1981) Nature 290, 161–163
20 Jacobs, R.E. and White, S.H. (1984) J. Am. Chem. Soc. 106, 915–920
21 Klason, T. and Henriksson, U. (1982) in Solution Behaviour of Surfactants (Mittal, K.L. and Fondler, E.J., eds.), p. 417, Plenum Press, New York
22 Seelig, J. and Neiderberger, W. (1974) Ber. Bunsenges. Phys. Chem. 78, 947–949
23 Ward, A.J.I., Friberg, S.E., Larsen, D.W. and Rananavare, S.B. (1984) J. Phys. Chem. 88, 826–827
24 Gruen, D.W.R. and Haydon, D.A. (1980) Biophys. J. 30, 129–136
25 Lee, A.G. (1976) Biochemistry 15, 2448–2454